	Eidgenössische	*Ecole polytechnique fédérale de Zurich*
ETH	**Technische Hochschule**	*Politecnico federale di Zurigo*
	Zürich	*Swiss Federal Institute of Technology Zurich*

Neumann-Neumann and FETI preconditioners for hp-approximations on geometrically refined boundary layer meshes in two dimensions*

A. Toselli and X. Vasseur

Neumann-Neumann and FETI preconditioners for hp-approximations on geometrically refined boundary layer meshes in two dimensions[*]

A. Toselli and X. Vasseur

Seminar für Angewandte Mathematik
Eidgenössische Technische Hochschule
CH-8092 Zürich
Switzerland

Abstract

We develop and analyze Neumann-Neumann and FETI methods for hp finite element approximations of scalar elliptic problems on geometrically refined boundary layer meshes in two dimensions. These are meshes that are highly anisotropic where the aspect ratio grows exponentially with the polynomial degree. The condition number is independent of the aspect ratio of the mesh and of potentially large jumps on the coefficients. In addition, it only grows polylogarithmically with the polynomial degree, as in the case of p approximations on shape-regular meshes.

Keywords: Domain decomposition, preconditioning, hp finite elements, spectral elements, anisotropic meshes

Subject Classification: 65N22, 65N55, 65N35

---

1 Introduction

It is well-known that solutions of elliptic boundary value problems in polyhedral domains have corner and edge singularities. In addition, boundary layers may also arise in laminar, viscous, incompressible flows with moderate Reynolds numbers at faces, edges, and corners. Suitably graded meshes, geometrically refined towards corners, edges, and/or faces, are required in order to achieve an exponential rate of convergence of hp finite element approximations; see, e.g., [2, 4, 28, 37, 38].

A typical case where boundary layers appear is given by the following diffusion-reaction problem

$$\begin{aligned} -\epsilon\nabla \cdot (\rho\nabla u) + u = f, &\quad \text{in } \Omega, \\ u = 0, &\quad \text{on } \partial\Omega, \end{aligned} \qquad (1)$$

where ϵ is a positive small parameter. Indeed, if f is not compatible with the boundary conditions, the problem does not have a solution for $\epsilon = 0$ and a boundary layer of width $\sqrt{\epsilon}$ is present along $\partial\Omega$ for ϵ small; see, e.g., [28].

In order to make the iterative solution of very large systems of finite element equations possible and efficient on parallel architectures, domain decomposition techniques (DD) have been used extensively in recent years; see the monographs [39, 33]. These methods are by now well-understood in various standard situations: with subdomains and meshes of regular shape, optimal or nearly optimal convergence of iterative solution techniques based on domain decomposition is by now well-established. This pertains to low order standard finite element discretizations as well as to high-order p-version or spectral element discretizations. In recent years there has also been some work for hp approximations; see [3, 1, 15, 6, 30, 16, 17] and the references therein.

Iterative substructuring methods rely on a non-overlapping partition into subdomains (substructures). Once the degrees of freedom inside the substructures have been eliminated by block Gaussian elimination, a preconditioner for the resulting Schur complement system is built with matrix blocks relative to a decomposition of interface finite element functions into subspaces related to geometrical objects (vertices, edges, faces, single substructures, ...). An iterative method like Conjugate Gradient is then employed.

Neumann-Neumann (NN) and Finite Element Tearing and Interconnecting (FETI) methods are among the most heavily tested iterative substructuring methods. As many others they in general share the property that the resulting condition number is independent of potentially large jumps of the coefficients across the substructures and only varies logarithmically with the number of degrees of freedom associated to each substructure, typically as a power of $\log(H/h)$ for the h version, $\log k$ for the p version or spectral elements, or $\log(kH/h)$ for the hp version. Here, H is the typical size of a substructure, h is the maximum diameter of the fine mesh, and k is the local polynomial degree of the finite element functions. Such bounds rely on certain Sobolev-type inequalities which are necessary to prove the stability of the relevant decompositions of

finite element functions; see section 7.2. NN and FETI methods present certain advantages over other iterative substructuring methods, like, for instance, the fact that the substructures do not need to form a coarse mesh but very general partitions can be considered, and that they can equivalently be employed for two and three dimensional problems.

Iterative substructuring methods generally require shape-regular subdomains and shape-regular and quasi-uniform meshes. Some work has been done for p approximations on thin domains, where one layer of very thin elements (which coincide with the subdomains in this case) can be employed. However the condition number may degrade very fast with the aspect ratio or these methods do not seem applicable to the case where the domain Ω is not thin and consequently many layers of thin elements are present; see [24, 22]. If substructures are not too thin but the local meshes are not quasi-uniform, the mesh size h in the ratio H/h must be replaced by the minimum of the diameters of the elements, thus giving a potentially large condition number if elements of very different size are employed. If in addition the local meshes are not shape-regular h must be in general replaced by the width of the thinnest element, thus giving very large condition numbers for meshes that are highly anisotropic.

All these remarks apply to the meshes that are commonly used for singularity and boundary layer resolution of hp approximations. Here we only consider two-dimensional meshes, which are described in detail in section 4. They are typically constructed from a shape-regular macro mesh $\mathcal{T}_m$, the elements of which are then geometrically refined towards the boundary with a grading factor $\sigma \in (0, 1)$ and a refinement level n; see Figure 2. The diameter of the smallest element and the width of the thinnest element are proportional to σ^n For singularity resolution only refinement towards the corners is necessary: the resulting mesh may not be in general quasi-uniform but it is still shape-regular (cf. Figure 2, right). For boundary layer resolution refinement towards the edges is also necessary, thus resulting in a highly anisotropic mesh (cf. Figure 2, left). According to our previous discussion, H/h is thus of the order of σ^{-n} in both cases. Since for exponential convergence n is chosen of the same order of k this would result in a condition number that grows at least as $\log(kH/h) \sim k \log k$ for a typical iterative substructuring method! Additional terms involving the aspect ratio of the fine mesh are also expected.

In this paper, we are able to derive efficient iterative substructuring methods for geometrically refined meshes, which still retain a polylogarithmic growth with k in the condition number. Indeed our meshes are highly anisotropic, but of a particular type:

1. they are obtained by refining an initial *shape-regular* coarse mesh;

2. refinement is only carried *towards* the boundary of the computational domain.

The analysis of iterative substructuring methods relies basically on two tools:

a. *stable decompositions* of finite element functions into terms associated to geometrical objects (in two dimensions typically vertices and edges, see Eq. (29));

b. *stable finite element extensions* of traces on the boundary of the substructures into the interior.

In view of these observations, we define our iterative substructuring methods in the following way:

i. We choose the macromesh as a decomposition into substructures in such a way that subdomains are shape-regular.

ii. The decomposition (29) only involves vertices which are far from the boundary and consequently the corresponding stability estimates only involve local quantities close to the internal vertices and far from the region where anisotropic refinement takes place: $(H/h) \sim (1 - \sigma)^{-1}$.

iii. Finding a stable finite element extension for local meshes that are not shape-regular or quasi-uniform is an open problem. However stable extensions are only employed in the analysis in order to compare the energy of functions on neighboring substructures with the same trace on the common boundary. This comparison can be carried out directly since our local meshes are of particular type; see section 7.3 and Figure 5 in particular.

We are then able to develop NN and FETI methods which provide a condition number that is independent on the refinement level n (and thus the aspect ratio of the fine mesh) and of potentially large jumps on the coefficients. In addition, our condition number bounds only grow quadratically with $\log k$, as is the case of p approximations on shape regular meshes. Such result should be compared with the condition number of the original stiffness matrix which is expected to grow *exponentially* with k: it grows at least as $k^3/(h_{min})^2 \sim k^3\sigma^{-2n} \sim k^3\sigma^{-2k}$, as is shown in [27] for shape-regular meshes and nodal basis functions on Gauss-Lobatto nodes.

We stress the fact that this is only a preliminary work and some important issues remain to be addressed. Some of them are discussed in section 11. Here we only mention that our analysis is only valid for two-dimensional problems and if nodal basis functions on Gauss-Lobatto nodes are employed. In addition, we only consider meshes without hanging nodes and the local problems on the substructures (macroelements) may be potentially large.

In this paper we will not carry on the analysis for the singularly-perturbed problem (1) but only consider the simplified problem

$$\begin{aligned} -\nabla \cdot (\rho \nabla u) &= f, \quad \text{in } \Omega, \\ u &= 0, \quad \text{on } \partial\Omega. \end{aligned} \tag{2}$$

We note that this problem does not have boundary layers but only corner singularities. We will then present some numerical results that indicate that the theoretical bounds proven also appear to hold for (1). An extensive numerical study is presented in [40].

The remainder of this paper is organized as follows: in sections 2 and 3, we introduce our continuous and discrete problems, respectively. Geometric boundary layer meshes are introduced in section 4. A particular choice of basis functions is given in section 5 and our domain decomposition preconditioners are defined in section 6. Section 7 is devoted to the proof of some important tools employed in our analysis. Theoretical bounds for NN and FETI methods are proved in sections 8 and 9, respectively. Some numerical experiments and concluding remarks are presented in section 10 and 11, respectively.

2 Problem setting

We consider a linear, elliptic problem on a bounded domain $\Omega \subset \mathbb{R}^2$ formulated variationally as:
Find $u \in H_0^1(\Omega)$, such that

$$a(u,v) = \int_\Omega \rho(x)\nabla u \cdot \nabla v \, dx = f(v), \quad v \in H_0^1(\Omega). \tag{3}$$

As usual, $H^1(\Omega)$ is the space of square summable functions with square summable first derivatives, and $H_0^1(\Omega)$ its subspace of functions that vanish on $\partial\Omega$. The functional $f(\cdot)$ belongs to the dual space $H^{-1}(\Omega)$.

The coefficient $\rho(x) > 0$ can be discontinuous, with very different values for different subregions, but we allow it to vary only moderately within each subregion. We will in fact assume that the region is the union of elements (also called subdomains, substructures, or macroelements) $\{\Omega_i\}$. More precise assumptions will be made in the following. Without decreasing the generality of our results, we will only consider the piecewise constant case:

$$\rho(x) = \rho_i, \quad x \in \Omega_i.$$

In the case of a region of diameter H_i, such as the substructure Ω_i, we use a norm with different relative weights obtained by a simple dilation argument:

$$\|u\|_{1,\Omega_i}^2 = |u|_{1,\Omega_i}^2 + \frac{1}{H_i^2}\|u\|_{0,\Omega_i}^2. \tag{4}$$

Here, $\|\cdot\|_{0,\Omega_i}$ and $|\cdot|_{1,\Omega_i}$ denote the norm in $L^2(\Omega_i)$ and the seminorm in $H^1(\Omega_i)$, respectively. In the following we also employ the space $W^{1,\infty}(\Omega_i)$ of bounded functions with bounded derivatives; see, e.g., [29].

3 hp finite element approximations

We now specify a particular choice of finite element spaces. Given an affine quadrilateral mesh $\mathcal{T}$ of Ω and a polynomial degree $k \geq 1$, we consider the following finite element spaces:

$$X = X^k(\Omega; \mathcal{T}) := \left\{ u \in H_0^1(\Omega) \,|\, \quad u_{|_K} \in \mathbb{Q}_k(K), \ K \in \mathcal{T} \right\}. \tag{5}$$

Here $\mathbb{Q}_k(K)$ is the space of polynomials of maximum degree k in each variable on K. In the following, we may drop the reference to k, Ω, and/or $\mathcal{T}$ whenever there is no confusion.

The mesh $\mathcal{T}$ is said to be *regular* or geometrically conforming if the intersection between neighboring elements is either a vertex or an entire edge of both elements. If hanging nodes are present it is called *irregular*; see, e.g., [35, 36]. We recall that conforming spaces can be defined on irregular meshes and, in order to do so, no degree of freedom is associated to a hanging node. In particular the degree of freedom of a basis function associated to such a node is constrained by the values of the basis functions on the other side; cf. Figure 2, right.

In this paper, we always assume that the meshes are regular. Irregular meshes with hanging nodes are commonly used in practice for hp approximations. However, we are unaware of any analysis of iterative substructuring methods for meshes with hanging nodes. If hanging nodes lie all in the interior of the subdomains, then our algorithms can be defined in a straightforward way, but the analysis does not appear to be trivial. If hanging nodes lie on the interface between the subdomains, then the definition of our algorithms is not unique; see section 6 for more comments.

A finite element approximation of (3) consists of finding $u \in X$, such that

$$a(u, v) = f(v), \quad v \in X. \tag{6}$$

4 Construction of geometric boundary layer meshes

In order to resolve boundary layers and/or singularities, geometrically graded meshes can be employed. They are determined by a mesh grading factor $\sigma \in (0, 1)$ and by the refinement level n. The number of layers is $n + 1$ and the thinnest layer has a width proportional to σ^n; see Figure 1. With an abuse of notation, we refer to n as the number of layers in the following. Robust exponential convergence of hp finite element approximations is achieved if n is suitably chosen. For singularity resolution, n is required to be proportional to the polynomial degree k; see [2, 4]. In the presence of boundary layers, the width of the thinnest layer needs to be comparable to that of the boundary layer; see [28, 37, 38]. In practical applications, for boundary layers of fixed width, and corner (and edge, in three dimensions) singularities, n is usually
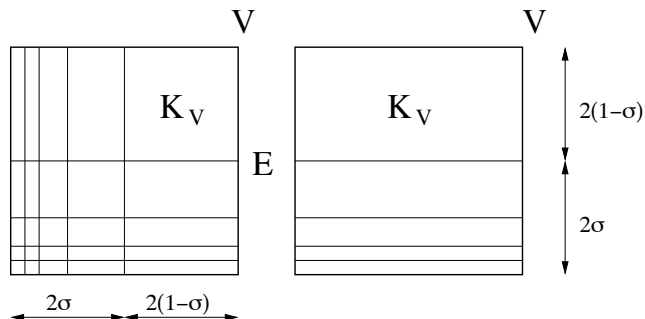
Figure 1: Corner and edge patches for boundary layer meshes on $\hat{Q}$ with $\sigma = 0.5$ and $n = 4$.

chosen proportional to the polynomial degree k, with the assumption that k is sufficiently large.

In this paper we only consider regular meshes. This means that we cannot treat meshes with hanging nodes which are often employed for singularity resolution when no boundary layer is present (geometrically refined corner meshes, cf. Figure 2, right). We note however that these meshes can also be employed for singularity resolution: they are regular, tensor product meshes which can be generated in a relatively simple and efficient way as opposed to irregular meshes with hanging nodes.

A two-dimensional geometric boundary layer mesh $\mathcal{T}_{bl}^{n,\sigma}$ is, roughly speaking, the tensor product of meshes that are geometrically refined towards the edges. Figure 2, left, shows an example of a boundary layer mesh.

The mesh $\mathcal{T}_{bl}^{n,\sigma}$ is built by first considering an initial shape-regular macro-triangulation $\mathcal{T}_m$ which is successively refined. Every macroelement can be refined isotropically, or anisotropically in order to obtain edge or corner patches as in Figure 1. Here and in the following, we only consider patches obtained by triangulating the reference square $\hat{Q} := I^2$, with $I := (-1, 1)$. A patch for an element $K_m \in \mathcal{T}_m$ is obtained by using an affine mapping $F_{K_m} : \hat{Q} \to K_m$.

An **edge patch** is given by an anisotropic triangulation of the form

$$\mathcal{T}_e := \{I \times K_y \mid \quad K_y \in \mathcal{T}_y\}, \tag{7}$$

where $\mathcal{T}_y$ is a mesh of I, geometrically refined towards, say $y = -1$, with grading factor $\sigma \in (0, 1)$ and n number of layers; see Figure 1, right, for a mesh with $\sigma = 0.5$ and $n = 4$.

A **corner patch** is given by an anisotropic triangulation of the form

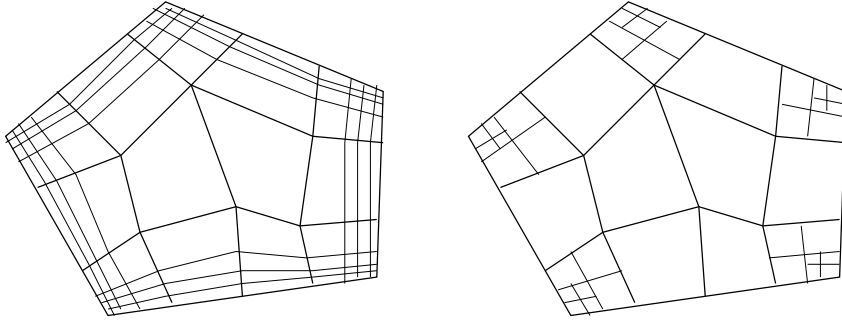$$\mathcal{T}_c := \{K_x \times K_y \mid \quad K_x \in \mathcal{T}_x, \ K_y \in \mathcal{T}_y\}, \tag{8}$$

Figure 2: Prototype boundary layer (left) and corner (right) meshes consisting of three types of patches. The macroelements are drawn with bold lines

where $\mathcal{T}_x$ and $\mathcal{T}_y$ are meshes of I, geometrically refined towards one vertex with a grading factor $\sigma \in (0,1)$ and number of layers n; see Figure 1, left.

The number of elements in an edge and corner patch with n layers is $O(n)$ and $O(n^2)$, respectively. Consequently, if $n = O(k)$, as is required for exponential convergence, the corresponding FE spaces have $O(k^3)$ and $O(k^4)$ degrees of freedom, respectively.

In the following, elements of meshes on the reference square $\hat{Q}$ will be denoted by $\hat{K}$. We note that every element $\hat{K}$ of $\mathcal{T}_e$ and $\mathcal{T}_c$ is of the form $(0, h_x) \times (0, h_y)$ (after a possible translation and rotation) and is thus obtained from the reference element by an affine mapping $F_{\hat{K}} : \hat{Q} \to \hat{K}$ of the form

$$[x \quad y]^T = [(h_x/2)(\hat{x} + 1) \quad (h_y/2)(\hat{y} + 1)]^T. \tag{9}$$

The aspect ratio of $\hat{K}$ is the maximum of the ratios h_x/h_y and h_y/h_x. Since the macromesh consists of affinely mapped elements K_m, every element K of the global mesh $\mathcal{T} = \mathcal{T}_{bl}^{n,\sigma}$ is obtained from the reference element by combining two affine mappings

$$K = F_K(\hat{Q}) = F_{K_m}(F_{\hat{K}}(\hat{Q})), \quad K \subset K_m \in \mathcal{T}_m. \tag{10}$$

Since $\mathcal{T}_m$ is shape-regular, the aspect ratio is determined by $F_{\hat{K}}$ only; cf. (9). Finally we note that the aspect ratio of the mesh is determined by σ and n, and is proportional to σ^{-n}.

Our analysis will be made for a prototype mesh, obtained from a shape-regular (not necessarily quasi-uniform) macromesh, by refining elements that touch $\partial\Omega$ only, either as corner or edge patches. Such meshes only consist of three types of patches: unrefined, edge, and corner patches; see Figure 2, left, for an example. We also recall that in practical applications σ is bounded away from one and zero.

5 Basis functions on Gauss-Lobatto nodes

We now introduce a particular nodal basis of $X^k(\Omega; \mathcal{T})$, where $\mathcal{T}$ is a geometric boundary layer mesh. Basis functions will be defined on the reference element and then mapped into the current element using (10). There are indeed technically two spaces: the space of finite element functions $X^k(\Omega; \mathcal{T})$ and the space of coefficients of these functions; we will make no distinction as far as notations are concerned.

We denote by $GLL(k)$ the set of Gauss-Lobatto points $\{\xi_i;\ 0 \leq i \leq k\}$ on $I = (-1, 1)$ in increasing order and by $\{w_i > 0\}$ the corresponding weights; see [5, Sect. 4]. For the square $\hat{Q} = (-1, 1)^2$ we set $GLL(k)^2 = \{\xi_{ij} = (\xi_i, \xi_j);\ 0 \leq i, j \leq k\}$ and denote by $\{w_{ij} = w_i w_j > 0\}$ the corresponding weights. We recall that $GLL(k)$ are the (distinct and real) zeros of $(1 - x^2)L'_{k-1}(x)$, with L_{k-1} the Legendre polynomial of degree $k - 1$ (cf. [5, Sect. 3]) and that the quadrature formula based on $GLL(k)$ has order $2k - 1$. In addition, we have

$$\|u\|^2_{L^2(I)} \leq \sum_{i=0}^{k} u(\xi_i)^2\, w_i \leq 3\, \|u\|^2_{L^2(I)}, \quad u \in \mathbb{Q}_k(I); \tag{11}$$

see [5, Rem. 13.3]. In the following, we use the same notation for the mapped Gauss-Lobatto nodes and corresponding weights for an affinely mapped element $K \in \mathcal{T}$. Similar estimates as (11) hold in two dimensions and for mapped elements.

Given the nodes $GLL(k)^2$, our basis functions on $\mathbb{Q}_k(\hat{Q})$ are the tensor product of k-th order Lagrange interpolating polynomials on $GLL(k)$, defined by

$$\hat{l}_i(\xi_j) = \delta_{ij}. \tag{12}$$

On the reference element we can write

$$u(x, y) = \sum_{i=0}^{k} \sum_{j=0}^{k} u(\xi_i, \xi_j)\, \hat{l}_i(x)\hat{l}_j(y), \quad u \in \mathbb{Q}_k(\hat{Q}). \tag{13}$$

For a general element in $\mathcal{T}$, basis functions are obtained by mapping those on the reference element. The local basis functions can be divided into *interior* (all local indices differ from 0 and k), *side* (only one of the indices is 0 or k), and *nodal* basis functions (all indices are 0 and/or k). We reserve the terms 'edge' and 'vertex' functions for subdomains; see below.

Equation (13) defines an interpolation operator I^k on the reference element

$$I^k u(x, y) := \sum_{i=0}^{k} \sum_{j=0}^{k} u(\xi_i, \xi_j)\, \hat{l}_i(x)\hat{l}_j(y);$$

it is clear that I^k can only be defined for continuous functions in general.

6 Iterative substructuring methods

Iterative substructuring methods
rely on a non-overlapping partition into substructures. We mention [39, Ch. 4]
as a general reference to this section. In our algorithms the substructures are
chosen as the macroelements in $\mathcal{T}_m = \{\Omega_i \mid 1 \leq i \leq N\}$. We recall that the
macroelements are shape regular. This appears to be essential for the analysis
and good performance. We refer to Figure 2, left, for an example. We also recall
that we only consider regular meshes; see Remark 6.1 for some comments.

We define the boundaries $\Gamma_i = \partial\Omega_i \setminus \partial\Omega$ and the interface Γ as their union.
We remark that Γ is the union of the interior subdomain *edges*, regarded as
open sets, which are shared by two subregions, and subdomain *vertices*, which
are shared by more than two subregions and can only be endpoints of edges.
We will always assume that points on $\partial\Omega$ are excluded and denote the edges
of Ω_i by E^{ik} and its vertices by V^{il}. Occasionally, we will also use edges and
vertices with one or no superscript.

When restricted to the subdomain Ω_i, the global triangulation $\mathcal{T}$ determines
a local mesh $\mathcal{T}_i$. This mesh can be of three types: edge, corner, or consisting
of just one element. We define the local spaces $X_i = X^k(\Omega_i; \mathcal{T}_i)$, of local finite
element functions that vanish on $\partial\Omega \cap \partial\Omega_i$, and the local bilinear forms

$$a_i(u,v) = \int_{\Omega_i} \rho_i \nabla u \cdot \nabla v \, dx, \quad u,v \in X_i.$$

We note that if Ω_i is a *floating* subdomain (i.e., its boundary does not touch
$\partial\Omega$), $a_i(\cdot, \cdot)$ is only positive semi-definite and for $u \in X_i$ we have

$$a_i(u,u) = 0 \quad \text{iff} \quad u \text{ constant in } \Omega_i.$$

The sets of nodal points on Γ_i, Γ, and E^{ik} are denoted by $\Gamma_{i,h}$, Γ_h, and E_h^{ik}
respectively. We will identify these sets with the corresponding sets of degrees
of freedom. As for the corresponding regions, we will also use notations with
one or no superscript. Recalling our terminology for local functions on single
elements, we note that the subdomain vertices V^{il} are element nodes, while the
nodal points in E_h^{ik} may correspond both to side and nodal functions.

We define some spaces defined on the interfaces: W_i is the space of restric-
tions to Γ_i of functions in $X^k(\Omega_i; \mathcal{T}_i)$ and W of restrictions to Γ of functions
in $X^k(\Omega; \mathcal{T})$. We note that functions in W_i and W are uniquely determined by
the nodal values in $\Gamma_{i,h}$ and Γ_h, respectively. For every substructure Ω_i, there
is a natural interpolation operator

$$R_i^T : W_i \longrightarrow W,$$

that extends a function on Γ_i to a global function on Γ with vanishing degrees of
freedom in $\Gamma_h \setminus \Gamma_{i,h}$. Its transpose with respect to the Euclidean scalar product
$R_i : W \to W_i$ extracts the degrees of freedom in $\Gamma_{i,h}$.

Once a vector $u \in X^k(\Omega; \mathcal{T})$ is expanded using the basis functions introduced in section 5, Problem (6) can be written as a linear system

$$Au = f.$$

We recall that the condition number of A is expected to grow at least as $k^3/(h_{min})^2 \sim k^3 \sigma^{-2n} \sim k^3 \sigma^{-2k}$ (see [27]) and may thus be extremely large for large values of k.

The contributions to the stiffness matrix and the right hand side can be formed one subdomain at a time. The stiffness matrix is then obtained by *subassembly* of these parts. We will order the nodal points interior to the subdomains first, followed by those on the interface Γ. Similarly, for the stiffness matrix relative to a substructure Ω_i, we have

$$A^{(i)} = \left(\begin{array}{cc} A_{II}^{(i)} & A_{I\Gamma}^{(i)} \\ A_{\Gamma I}^{(i)} & A_{\Gamma\Gamma}^{(i)} \end{array} \right).$$

In a first step of many iterative substructuring algorithms, the unknowns in the interior of the subdomains are eliminated by block gaussian elimination. In this step, the Schur complements, with respect to the variables associated with the boundaries of the individual substructures, are calculated. The resulting linear system can be written as

$$S u_\Gamma = g_\Gamma. \tag{14}$$

Given the local Schur complements

$$S_i = A_{\Gamma\Gamma}^{(i)} - A_{I\Gamma}^{(i)^T} A_{II}^{(i)^{-1}} A_{I\Gamma}^{(i)} : W_i \longrightarrow W_i,$$

we have

$$S = \sum_{i=1}^N R_i^T S_i R_i : W \longrightarrow W$$

and an analogous formula can be found for g_Γ; see [39, Ch. 4].

A function $u^{(i)}$ defined on Ω_i is said to be discrete harmonic on Ω_i if

$$A_{II}^{(i)} u_I^{(i)} + A_{I\Gamma}^{(i)} u_\Gamma^{(i)} = 0.$$

In this case, it is easy to see that $\mathcal{H}_i(u_\Gamma^{(i)}) := u^{(i)}$ is completely defined by its value on Γ_i. The space of piecewise discrete harmonic functions u consists of functions in X that are discrete harmonic on each substructure. In this case, $u =: \mathcal{H}(u_\Gamma)$ is completely defined by its value on Γ.

Our preconditioners will be defined with respect to the inner product

$$s(u, v) = u^T S v, \quad u, v \in W.$$

It follows immediately from the definition of S that $s(\cdot, \cdot)$ is symmetric and coercive.

The following lemma results from elementary variational arguments.

Lemma 6.1 *Let $u_\Gamma^{(i)}$ be the restriction of a finite element function to Γ_i. Then the discrete harmonic extension $u^{(i)} = \mathcal{H}_i(u_\Gamma^{(i)})$ of $u_\Gamma^{(i)}$ into Ω_i satisfies*

$$a_i(u^{(i)}, u^{(i)}) = \min_{v^{(i)}|_{\partial\Omega_i} = u_\Gamma^{(i)}} a_i(v^{(i)}, v^{(i)}) = u_\Gamma^{(i)^T} S^{(i)} u_\Gamma^{(i)}.$$

Analogously, if u_Γ is the restriction of a finite element function to Γ, the piecewise discrete harmonic extension $u = \mathcal{H}(u_\Gamma)$ of u_Γ into the interior of the subdomains satisfies

$$a(u, u) = \min_{v|_\Gamma = u_\Gamma} a(v, v) = s(u, u) = u_\Gamma^T S u_\Gamma.$$

This lemma ensures that instead of working with functions defined on the interface Γ, we can equivalently work with the corresponding discrete harmonic extensions. For this reason, in the following we will identify spaces of traces on the interfaces, W_i and W, with spaces of discrete harmonic extensions. We point out however that due to the particular meshes considered, we cannot equivalently work with norms of local discrete harmonic extensions and traces on the subdomain boundaries since our local meshes are not in general quasi-uniform or shape-regular, and stable discrete harmonic extensions cannot be found in general.

6.1 Neumann-Neumann methods

Neumann-Neumann methods provide preconditioners for the Schur complement system: instead of solving (14) using, e.g., the conjugate gradient method, they employ an equivalent system involving a preconditioned operator of the form

$$\hat{S}^{-1} S = P_{NN} = P_0 + (I - P_0)(\sum_{i=1}^N P_i)(I - P_0).$$

We refer to [11, 23, 31, 19] for some NN methods for the h and p finite elements. We are unaware on any such method for hp approximations.

The operators P_i are projection-like operators associated to a family of subspaces W_i and determined by a set of local bilinear forms defined on them

$$\tilde{s}_i(u, v), \quad u, v \in W_i.$$

Given interpolation operators $R_i^T : W_i \to W$, we have

$$P_i = R_i^T \tilde{P}_i, \quad \tilde{P}_i : W \longrightarrow W_i, \tag{15}$$

with

$$\tilde{s}_i(\tilde{P}_i u, v_i) = s(u, R_i^T v_i), \quad v_i \in W_i. \tag{16}$$

12

While P_0 is associated to a low-dimensional global problem, the others are associated to the single substructures. The remainder of this section is devoted to the definition of the various components of P_{NN}.

An important role is played by a family of weighted counting functions δ_i, which are associated with and defined on the individual Γ_i (cf. [9, 11, 23, 34, 31]) and are defined for $\gamma \in [1/2, \infty)$. Given Ω_i and $x \in \Gamma_{i,h}$, $\delta_i(x)$ is determined by a sum of contributions from Ω_i and its relevant next neighbors,

$$\delta_i(x) = \sum_{j \in \mathcal{N}_x} \rho_j^\gamma(x)/\rho_i^\gamma(x), \quad x \in \Gamma_{i,h}. \tag{17}$$

Here $\mathcal{N}_x$, $x \in \Gamma_h$, is the set of indices j of the subregions such that $x \in \Gamma_{j,h}$. The function δ_i is discrete harmonic and thus belongs to W_i. The pseudoinverses $\delta_i^\dagger \in W_i$ are defined, for $x \in \Gamma_{i,h}$, by

$$\delta_i^\dagger(x) = \delta_i^{-1}(x), \quad x \in \Gamma_{i,h}. \tag{18}$$

We note that these functions provide a partition of unity:

$$\sum_{i=1}^N R_i^T \delta_i^\dagger(x) \equiv 1. \tag{19}$$

In particular, for $u \in W$ we can use the formula

$$u = \sum_{i=1}^N R_i^T u_i, \quad \text{with } u_i = \mathcal{H}_i(\delta_i^\dagger u). \tag{20}$$

Here and from now on, we will tacitly assume that whenever we write $\mathcal{H}_i(uv)$ or $\mathcal{H}(uv)$ we first form $I^k(uv)$, i.e., map the product of the two functions u and v into the finite element space by interpolation, and then extend the result as a discrete harmonic function.

Our coarse space W_0 is defined as

$$W_0 = \text{span}\{R_i^T \delta_i^\dagger\} \subset W,$$

where the span is taken over the floating subdomains. We note that W_0 consists of piecewise discrete harmonic functions and R_0^T is the natural injection $W_0 \subset W$. We consider an exact solver on W_0

$$\tilde{s}_0(u, v) := a(\mathcal{H}u, \mathcal{H}v) = a(u, v).$$

For every substructure Ω_i the local bilinear form is

$$\tilde{s}_i(u, v) := a_i(\mathcal{H}_i(\delta_i u), \mathcal{H}_i(\delta_i v)), \quad u, v \in W_i.$$

For a floating subdomain $\tilde{P}_i$ is defined only for those $u \in W$ for which $s(u, v) = 0$ for all $v = R_i^T v_i$ such that $\mathcal{H}_i(\delta_i v_i)$ is constant on Ω_i. This condition is satisfied

if $a(u, R_i^T \delta_i^\dagger) = 0$; we note that this test function is a basis function for W_0. For such subdomains, we make the solution $\tilde{P}_i u$ of (16) unique by imposing the constraint

$$\int_{\Omega_i} \mathcal{H}_i(\delta_i \tilde{P}_i u) dx = 0, \tag{21}$$

which just means that we select the solution orthogonal to the null space of the Neumann operator. Thus, $Range(\tilde{P}_i)$ has codimension 1 with respect to the space W_i.

We can equally well use matrix notations. Let D_i be the diagonal matrix with the elements $\delta_i^\dagger(x)$ corresponding to the point $x \in \Gamma_{i,h}$. Then

$$\tilde{s}_i(u, v) = u^T D_i^{-1} S_i D_i^{-1} v.$$

We also have,

$$P_i = R_i^T D_i S_i^\dagger D_i R_i S,$$

where $S_i^\dagger$ is a pseudoinverse of S_i. Analogously for the coarse projection

$$P_0 = R_0^T S_0^{-1} R_0 S,$$

where $S_0 = R_0 S R_0^T$ the restriction of S to W_0

One of the main results of this paper is a bound for the condition number of P_{NN}. Such bound can be found using the abstract Schwarz theory; see, e.g., [39, Ch. 6]. We refer to [23, 11, 31, 39, 19] for similar proofs.

A uniform bound for the smallest eigenvalue can be found using the decomposition (20) and the fact that P_0 is an orthogonal projection.

Lemma 6.2 *We have*

$$s(P_{NN}u, u) \geq s(u, u), \quad u \in W.$$

In order to find a bound for the largest eigenvalue, we need a stability property for the local bilinear forms; see, e.g., [39].

Assumption 6.1 *We have*

$$s(R_i^T u_i, R_i^T u_i) \leq \omega \, \tilde{s}_i(u_i, u_i), \qquad u_i \in Range(\tilde{P}_i), \quad i = 1, \cdots, N,$$

with

$$\omega = C \, (1 - \sigma)^{-4} \left(1 + \log\left(\frac{k}{1 - \sigma}\right) \right)^2$$

and C independent of k, n, σ, γ, the coefficients ρ_i, and the diameters H_i.

The proof of Assumption 6.1 is given in section 8. Assumption 6.1 and a coloring argument provide a bound for the largest eigenvalue; see, e.g., [32, Sect. 8].

Lemma 6.3 *Let Assumption 6.1 be satisfied. Then*

$$s(P_{NN}u, u) \le C\omega s(u, u), \quad u \in W.$$

Consequently the condition number of P_{NN} satisfies

$$\kappa(P_{NN}) \le C\omega = C(1 - \sigma)^{-4} \left(1 + \log\left(\frac{k}{1 - \sigma}\right)\right)^2.$$

Remark 6.1 *We note that our Neumann-Neumann algorithm can still be defined for irregular meshes with hanging nodes that lie in the interior of the substructures. The analysis however does not appear to be trivial; in particular we cannot exploit the equivalence of polynomials and bilinear functions on Gauss-Lobatto meshes as in section 7.1. Other iterative substructuring methods for hp approximations also seem to require regular meshes; see [3, 24, 22, 1, 15, 6, 30, 16, 17]. If hanging nodes are present on the interface Γ, then there is no straightforward way of defining a Neumann-Neumann algorithm. For the definition of W_i, we can choose for instance the restriction of functions in W to Γ_i (and thus no* local *degree of freedom is associated to a hanging node), or we can associate local degrees of freedom to hanging nodes (the definition of the extension R_i^t is thus not straightforward). Whatever the choice, it does not appear to be trivial to define the weighting counting functions δ_i in such a way that, for instance, the decomposition (20) still holds. For these reasons we leave the important case of irregular meshes to a future work.*

6.2 One-level FETI methods

FETI methods were first introduced in [14]. Since then, considerable work has been done on FETI methods and many variants and improvements have been proposed. We refer to [13] for a detailed introduction and to [25, 19] for the analysis of one-level FETI methods

Instead of solving the Schur complement system (14) directly, we work with a space of discontinuous functions across the interface Γ

$$\tilde{W} = \prod_{i=1}^{N} W_i.$$

For $u \in \tilde{W}$, let u_i be its component associated to W_i. We consider the equivalent constrained problem: find $u \in \tilde{W}$, such that

$$\left. \begin{array}{c} J(u) := \frac{1}{2} u^T \tilde{S} u - \tilde{f}^T u \to \min \\ Bu = 0 \end{array} \right\}. \tag{22}$$

Here, the matrix $B = [B_1, B_2, \ldots, B_N]$ is constructed from $\{0, 1, -1\}$ such that the values of the solution u associated with more than one subdomain coincide

when $Bu = 0$. We note that the choice of B is far from unique. The matrix $\tilde{S}$ is a block diagonal matrix constructed with the local Schur complements S_i. We recall that S_i is singular if and only if Ω_i is a floating subdomain. By introducing a vector of Lagrange multipliers λ to enforce the constraints $Bu = 0$, we obtain a saddle point formulation of (22): find $(u, \lambda) \in W \times U$ such that

$$\left. \begin{array}{r} \tilde{S}u + B^T \lambda = \tilde{f} \\ Bu = 0 \end{array} \right\} \tag{23}$$

with $U = Range(B)$. In this work we only consider the case of non-redundant Lagrange multipliers, i.e., when no redundant condition is imposed by $Bu = 0$, and thus B has full rank. We refer to, e.g., [19] for other variants and additional comments; here we only note that the case of redundant Lagrange multipliers can also be employed and analyzed for our problem.

In the next step we eliminate the primal variable u. Since $\tilde{S}$ is singular, we need to employ a pseudoinverse $\tilde{S}^\dagger$, constructed with pseudoinverses of local Neumann problems $S_i^\dagger$. In addition we introduce the full-column rank matrix R built from all the null space elements of $\tilde{S}$

$$R = \begin{bmatrix} r_1 & O & \cdots & O \\ O & r_2 & \ddots & \vdots \\ \vdots & \ddots & \ddots & O \\ O & \cdots & O & r_N \end{bmatrix}.$$

We have $Range(R) = Kernel(\tilde{S})$. In fact, the subdomains that intersect $\partial\Omega$ do not contribute to $Kernel(\tilde{S})$, and therefore those columns of R are void, while for a floating substructure we can choose a vector of all ones. We find

$$u = \tilde{S}^\dagger(\tilde{f} - B^T\lambda) + R\alpha, \quad (\tilde{f} - B^T\lambda) \perp Kernel(\tilde{S}).$$

We thus obtain

$$\left. \begin{array}{rcl} F\lambda - G\alpha & = & d \\ G^T\lambda & = & e \end{array} \right\} \tag{24}$$

with $F := B\tilde{S}^\dagger B^T$, $G := BR$, $d := B\tilde{S}^\dagger\tilde{f}$, and $e := R^T\tilde{f}$.

We now introduce a symmetric, positive definite matrix Q and define an inner product $\langle \lambda, \mu \rangle_Q := \langle \lambda, Q\mu \rangle$ on $U = Range(B)$. Here $\langle \cdot, \cdot \rangle$ stands for the Euclidean inner product. Let $P^T := I - G(G^TQG)^{-1}G^TQ$. We find that

$$\left. \begin{array}{r} P^TF\lambda = P^Td \\ G^T\lambda = e \end{array} \right\} \tag{25}$$

We note that P is an orthogonal projection from U onto $Kernel(G^T)$; this projection is orthogonal in the Q^{-1} inner product, i.e., the inner product defined

by $\langle \lambda, Q^{-1}\mu \rangle$. We introduce the subspace

$$V := \{\lambda \in U \,:\, \langle \lambda, Bz \rangle = 0, \quad z \in Kernel(S)\} = Kernel(G^T) = Range(P). \tag{26}$$

The one-level FETI method is a preconditioned conjugate gradient method, in the space V, applied to the first one of (25) with an initial approximation λ_0 chosen such that $G^T\lambda_0 = e$:

$$PM^{-1}P^T F\lambda = PM^{-1}P^T d, \quad \lambda \in \lambda_0 + V. \tag{27}$$

Many choices have been proposed for the preconditioner M^{-1} and the matrix Q. The choice

$$M^{-1} := (BD^{-1}B^T)^{-1}BD^{-1}SD^{-1}B^T(BD^{-1}B^T)^{-1}, \quad Q := M^{-1}$$

provides a condition number that is independent of the ρ_i; see [19]. Here $D : \tilde{W} \to \tilde{W}$ is a block diagonal matrix: each block, corresponding to one substructure, is equal to D_i, the local scaling matrix introduced in the previous section. We note that $(BD^{-1}B^T)$ is block diagonal and each block corresponds to one node in $\Gamma_{i,h}$, the size of which equals the number of conditions associated to that node in $Bu = 0$. We note that M^{-1} does not have an inverse but that PM^{-1} is a one-to-one mapping from $Range(P^T)$ to $V = Range(P)$.

A uniform bound for the smallest eigenvalue of the preconditioned operator can be found using simple linear algebra arguments; see, e.g, [25].

Lemma 6.4 *We have*

$$\langle F\lambda, \lambda \rangle \geq \langle M\lambda, \lambda \rangle, \quad \lambda \in V.$$

In order to find a bound for the largest eigenvalue, it is convenient to introduce the jump operator

$$P_D := D^{-1}B^T(BD^{-1}B^T)^{-1}B, \tag{28}$$

which maps $\tilde{W}$ into itself.

We require a stability property for P_D; see, e.g., [19].

Assumption 6.2 *We have*

$$|P_D u|_{\tilde{S}}^2 \leq \omega |u|_{\tilde{S}}^2, \quad u \in Range(\tilde{S}),$$

where

$$|u|_{\tilde{S}}^2 := \langle u, \tilde{S}u \rangle = \sum_{i=1}^{N} \langle u_i, S_i u_i \rangle = \sum_{i=1}^{N} a_i(\mathcal{H}_i u_i, \mathcal{H}_i u_i) = \sum_{i=1}^{N} a_i(u_i, u_i), \quad u \in \tilde{W}$$

and ω is the same as in Assumption 6.1.

The proof of Assumption 6.2 is given in section 9. Assumption 6.2 and simple linear algebra arguments provide a bound for the largest eigenvalue; see [19, Th. 1].

Lemma 6.5 *Let Assumption 6.2 be satisfied. Then*

$$\langle F\lambda, \lambda \rangle \leq \omega \langle M\lambda, \lambda \rangle, \quad \lambda \in V.$$

Consequently the condition number of the preconditioned FETI operator satisfies

$$\kappa(PM^{-1}P^T F) \leq \omega = C\,(1-\sigma)^{-4}\left(1 + \log\left(\frac{k}{1-\sigma}\right)\right)^2.$$

Remark 6.2 *A new class of FETI methods has recently been introduced, the so-called dual-primal FETI methods; see [12]. In two dimensions variables associated to the vertices of the substructures are eliminated together with the internal degrees of freedom. The constrained problem in (22) only involves degrees of freedom in the interior of the edges of the subdomains and the resulting Schur complement $\tilde{S}$ is invertible. An equation for the Lagrange multiplier λ is then obtained: $F\lambda = d$, cf. (24). The same preconditioner M^{-1} is employed and the preconditioned operator $M^{-1}F$ has the same condition number bound as for one-level FETI methods. We refer to [26, 20] for the analysis of certain dual primal FETI methods. These methods can be defined for our approximations as well and the proof can be carried out as in [26, 20].*

7 Technical Tools

7.1 Gauss-Lobatto meshes

We now introduce an additional refined mesh based on the Gauss-Lobatto points on each element of $\mathcal{T}$. It will be a useful tool for the proof of certain properties. These results are well known and can be found in [5, 7, 8].

The points $GLL(k)^2$ define a triangulation $\mathcal{T}_k = \mathcal{T}_k(\hat{Q})$ of $\hat{Q}$ in a natural way, consisting of k^2 rectangles. Let $Y^h = Y^h(\hat{Q}) = X^1(\hat{Q}; \mathcal{T}_k)$ be the space of piecewise bilinear functions on this mesh. We also denote $Y^k = Y^k(\hat{Q}) = \mathbb{Q}_k(\hat{Q})$. The aspect ratio of $\mathcal{T}_k$ is of the order of k; see [8, Pg. 27] for details. In a similar way we can consider a Gauss-Lobatto mesh on an affinely mapped element K by simply mapping the mesh on $\hat{Q}$. In the following, we will use the notations $\mathcal{T}_k = \mathcal{T}_k(K)$, $Y^h = Y^h(K)$, and $Y^k = Y^k(K)$, to denote the GL mesh, the piecewise bilinear finite element space, and $\mathbb{Q}_k$, respectively, for a mapped element. If the aspect ratio of K is, e.g., h_x/h_y (cf. (9) and (10)), then that of the corresponding $\mathcal{T}_k$ is $(h_x/h_y)k$. We refer to Figure 3 for an example.

There is a one-to-one correspondence between Y^h and Y^k given by
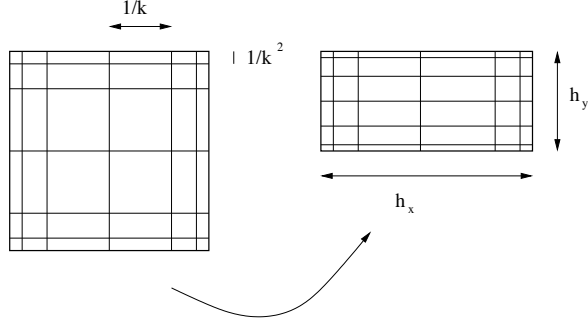
$$I^k : Y^h \to Y^k, \quad I^h : Y^k \to Y^h,$$

Figure 3: Gauss-Lobatto meshes on a reference and a stretched element

where I^h is the nodal interpolation operator on Y^h. We use the notation $u_h \in Y^h$ and $u_k \in Y^k$ in order to denote two corresponding functions.

Lemma 7.1 *Let* $\hat{K} = (0, h_x) \times (0, h_y)$. *Then there exist positive constants* c *and* C, *such that, for* $u_h \in Y^h(\hat{K})$,

$$c\|u_h\|_{0,\hat{K}} \leq \|u_k\|_{0,\hat{K}} \leq C\|u_h\|_{0,\hat{K}},$$
$$c\|\partial_x(u_h)\|_{0,\hat{K}} \leq \|\partial_x(u_k)\|_{0,\hat{K}} \leq C\|\partial_x(u_h)\|_{0,\hat{K}},$$
$$c\|\partial_y(u_h)\|_{0,\hat{K}} \leq \|\partial_y(u_k)\|_{0,\hat{K}} \leq C\|\partial_y(u_h)\|_{0,\hat{K}},$$

with, in particular, c *and* C *independent of* h_x, h_y, *and* k. *If* $K \in \mathcal{T}$ *is given by (10), then, for* $u_h \in Y^h(K)$,

$$c\|u_h\|_{0,K} \leq \|u_k\|_{0,K} \leq C\|u_h\|_{0,K},$$
$$c|u_h|_{1,K} \leq |u_k|_{1,K} \leq C|u_h|_{1,K}$$

where the constants are independent of the diameter and the aspect ratio of K, *and* k.

The proof of the result above can be found in [7, Sect. 2] for $K = \hat{Q}$. For an affinely mapped element a scaling argument can be then used. We note that thanks to Lemma 7.1 we can equivalently work with functions in Y^k or Y^h.

The following result can be found in [8, Lem. 3.3.2].

Lemma 7.2 *Let* $\hat{K} = (0, h_x) \times (0, h_y)$ *and* $u_h \in Y^h(\hat{K})$. *Given* $\theta \in W^{1,\infty}(\hat{K})$, *with*

$$\|\theta\|_{\infty,\hat{K}} \leq C, \quad \|\nabla\theta\|_{\infty,\hat{K}} \leq C/r,$$

then

$$\|I^h(\theta u_h)\|^2_{0,\hat{K}} \leq C\|u_h\|^2_{0,\hat{K}},$$
$$\|\partial_x I^h(\theta u_h)\|^2_{0,\hat{K}} \leq C(|u_h|^2_{1,\hat{K}} + r^{-2}\|u_h\|^2_{0,\hat{K}}),$$

where C is independent of h_x, h_y, and k. A similar bound holds for the y-derivative. If $K \in \mathcal{T}$ is given by (10), then, for $u_h \in Y^h(K)$,

$$\|I^h(\theta u_h)\|_{0,K}^2 \le C\|u_h\|_{0,K}^2,$$
$$|I^h(\theta u_h)|_{1,K}^2 \le C(|u_h|_{1,K}^2 + r^{-2}\|u_h\|_{0,K}^2),$$

where C is independent of the diameter and the aspect ratio of K, and k.

Given an element $\hat{K} = (0, h_x) \times (0, h_y)$, let $a = (0,0)$ and $b = (h_x, 0)$ and a' and b' be the corresponding vertices on the parallel edge. In addition, if $d = (0,0)$ and $e = (0, h_y)$, let d' and e' be the corresponding vertices on the parallel edge. The following lemma relies on trivial properties of bilinear functions; cf. [8, Lem. 3.3.1].

Lemma 7.3 *Let $\hat{K} = (0, h_x) \times (0, h_y)$. Then there are constants independent of h_x and h_y, such that, if u is bilinear on $\hat{K}$,*

$$c\|u\|_{0,\hat{K}}^2 \le h_x h_y \sum_{x=a,b} (u(x)^2 + u(x')^2) \le C\|u\|_{0,\hat{K}}^2,$$
$$c\|\partial_x u\|_{0,\hat{K}}^2 \le (h_y/h_x) \sum_{x=a,b} (u(x) - u(x'))^2 \le C\|\partial_x u\|_{0,\hat{K}}^2,$$
$$c\|\partial_y u\|_{0,\hat{K}}^2 \le (h_x/h_y) \sum_{x=d,e} (u(x) - u(x'))^2 \le C\|\partial_y u\|_{0,\hat{K}}^2,$$
$$c\|\partial_x u\|_{\infty,\hat{K}}^2 \le h_x^{-2} \sum_{x=a,b} (u(x) - u(x'))^2 \le C\|\partial_x u\|_{\infty,\hat{K}}^2,$$
$$c\|\partial_y u\|_{\infty,\hat{K}}^2 \le h_y^{-2} \sum_{x=d,e} (u(x) - u(x'))^2 \le C\|\partial_y u\|_{\infty,\hat{K}}^2$$

7.2 Decomposition results

One of the key ingredients for the proof of Assumptions 6.1 and 6.2, and for the analysis of many iterative substructuring methods is a decomposition result for local functions in W_i into edge and vertex components:

$$u = \sum_k u_{E^{ik}} + \sum_l u_{V^{il}}, \quad u \in W_i. \tag{29}$$

The edge component $u_{E^{ik}}$ vanishes on $\partial\Omega_i \setminus E^{ik}$ and is discrete harmonic. It is uniquely determined by the nodal values in E_h^{ik}. The vertex component $u_{V^{il}}$ is also discrete harmonic and vanishes at all points of $\Gamma_{i,h}$ except V^{il}; the value of the function at V^{il} uniquely determines it:

$$u_{V^{il}}(x) = u(V^{il}) \, \phi_{V^{il}}(x),$$

where $\phi_{V^{il}} \in W_i$ is one at V^{il} and zero at the remaining points of $\Gamma_{i,h}$.

Here and in the following section we only carry out proofs for the reference square $\hat{Q}$: since elements in the macromesh $\mathcal{T}_m$ are shape-regular and affinely

mapped, the corresponding bounds for a generic substructure $\Omega_i \in \mathcal{T}_m$, of diameter H_i, can be obtained by a standard scaling argument and involve the scaled norm (4).

We first consider the vertex components. We recall that we only need to consider three types of patches: edge, corner, and unrefined ones, together with the corresponding triangulations $\mathcal{T}_e$, $\mathcal{T}_c$, and $\hat{Q}$, respectively; cf. Figures 1 and 2. A generic patch is denoted by Ω_i and its triangulation by $\mathcal{T}_i$. Let V be a vertex of Ω_i that does not lie on $\partial\Omega$. There is a unique element $K_V \in \mathcal{T}_i$ to which this vertex belongs. We note that the aspect ratio of K_V is independent of the refinement level n: it is bounded by a constant C for the case of a corner and unrefined patch, while it is bounded by $C(1-\sigma)^{-1}$ for an edge patch; see Figure 1.

We next consider the Gauss-Lobatto mesh $\mathcal{T}_k(K_V)$ on K_V and assume that V belongs to $k_V \in \mathcal{T}_k(K_V)$. We note that the aspect ratio of k_V satisfies a similar bound as for K_V; see Figure 3.

Lemma 7.4 *Let $u_V \in W_i$ be discrete harmonic and vanish at all nodal points $\Gamma_{i,h}$ except at the vertex V. Then there is a constant independent of u_V, H_i, σ, and n, such that*

$$|u_V|^2_{1,\Omega_i} \le C(1-\sigma)^{-1}|u_V(V)|^2 \le C(1-\sigma)^{-1}\|u_V\|^2_{\infty,K_V}.$$

Proof. We only consider the worst possible case, i.e., that of an edge patch, for which, after a possible translation and rotation,

$$k_V = (0, Ck^{-2}(1-\sigma)) \times (0, Ck^{-2});$$

cf. Figure 1, right. The result follows by estimating the energy norm of the zero extension of the boundary values and by noting that the harmonic extension has a smaller energy (cf. Lemma 6.1). More precisely, let u_k be the function that vanishes at all nodal points in $\Omega_{i,h} \cup \Gamma_{i,h}$ except at V and $u_h = I^h u_k$ the corresponding piecewise bilinear function defined on the Gauss-Lobatto mesh. Using Lemma 7.3, we find

$$\|\nabla u_h\|_{\infty,k_V} \le C\,|u_V(V)|\,k^2(1-\sigma)^{-1}.$$

Since the area of k_V is bounded by $Ck^{-4}(1-\sigma)$, we find

$$|u_h|^2_{1,\Omega_i} = |u_h|^2_{1,k_V} \le C\,\|\nabla u_h\|^2_{\infty,k_V} \cdot k^{-4}(1-\sigma) = C(1-\sigma)^{-1}|u_V(V)|^2.$$

A bound for u_k is then obtained using Lemma 7.1. $\square$

We now have a bound for vertex components.

Theorem 7.1 *Let $u \in W_i$ and u_V its component relative to a vertex V. Then there is a constant independent of u, H_i, σ, and n, such that*

$$|u_V|^2_{1,\Omega_i} \le C(1-\sigma)^{-1}|u(V)|^2 \le C(1-\sigma)^{-1}\|u\|^2_{\infty,K_V}.$$

A complementary result is given by the inverse estimate in the following lemma.

Lemma 7.5 *Let $u \in X_i$. Then there is a constant independent of u, H_i, σ, and n, such that*

$$|u(V)|^2 \leq \|u\|_{\infty,K_V}^2 \leq C\,(1-\sigma)^{-2}\,(1+\log k)\,\|u\|_{1,K_V}^2.$$

Proof. Due to the presence of the full H^1-norm, the worst case is here for the corner patch, for which, after a possible translation, we have

$$K_V = (0, C(1-\sigma)) \times (0, C(1-\sigma));$$

cf. Figure 1, left. Let $K_V = F_{K_V}(\hat{Q})$ with F_{K_V}, an affine mapping. On the reference element $\hat{Q}$, [37, Th. 4.76] gives

$$\|u\|_{\infty,\hat{Q}}^2 \leq C\,(1+\log k)\,\|u\|_{1,\hat{Q}}^2.$$

The proof is then concluded by using the mapping $K_V = F_{K_V}(\hat{Q})$. □

We next consider the edge contributions of the decomposition (29). Bounds for the unrefined patch follow from standard results for spectral elements. For the edge and corner patch, we employ a cut-off function θ_E and Lemma 7.2. We note that we need to consider one possible case for the corner patch and two for the edge patch; cf. Figure 1. Here we only consider the edge patch: the corner patch can be treated in a similar way.

Lemma 7.6 *Given an edge E^j of Ω_i, there exists a continuous function θ_{E^j}, defined on $\overline{\Omega_i}$, that is equal to one at the nodal points of E_h^j and zero on $\Gamma_{i,h} \backslash E_h^j$, such that*

$$\begin{aligned} 0 &\leq \theta_{E^j} \leq 1, \\ |\nabla \theta_{E^j}| &\leq C/r, \end{aligned} \tag{30}$$

where $r = r(x,y)$ is the distance to the closest vertex of Ω_i that does not lie on $\partial\Omega$.

Proof. We only consider the case of an edge patch on $\hat{Q}$ in full detail. The bounds for a generic substructures are obtained by a scaling argument.

We consider the configuration in Figure 4 and assume that the edge E^4 ($y = -1$) lies on $\partial\Omega$. We only need to construct three functions. We start by constructing functions ϑ_{E^j} which we will then interpolate. We divide $\hat{Q}$ into eight triangles by connecting the center $C = (0,0)$ to all the vertices and to the four centers C^j of the edges.

We first assign values in the upper rectangle $y \geq 0$:
The function ϑ_{E^j} is equal to $1/3$ at the center C and at the centers of the edges $\vartheta_{E^j}(C^l) = \delta_{jl}$. They are then linear functions along each segment CC^j. The value inside a triangle determined by CC^j and a vertex of E^j is constant along
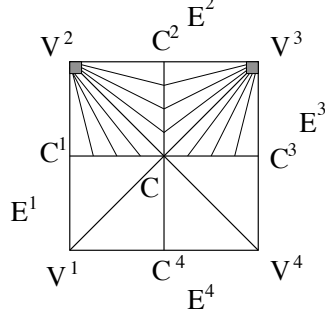
Figure 4: Construction of the functions ϑ_{E^j}, $j = 1, 2, 3$, on an edge patch. The lines inside the triangles are lines where the ϑ_{E^j} are constant

any straight line through that vertex and is given by the value, already known, on the segment CC^j. We note that this procedure determines the ϑ_{E^j} at all points with $y \geq 0$, except at the two vertices V^2 and V^3; cf. Figure 4. For $y \leq 0$ we assign values at the two lower vertices V^1 and V^4 and the center C^4. We then interpolate linearly on the four lower triangles. We set

$$
\begin{array}{lll}
\vartheta_{E^1}(V^1) = 1, & \vartheta_{E^1}(V^4) = 0, & \vartheta_{E^1}(C^4) = 1/2, \\
\vartheta_{E^3}(V^1) = 0, & \vartheta_{E^3}(V^4) = 1, & \vartheta_{E^3}(C^4) = 1/2, \\
\vartheta_{E^2}(V^1) = 0, & \vartheta_{E^1}(V^4) = 0, & \vartheta_{E^2}(C^4) = 0.
\end{array}
$$

We next consider the triangulation $\mathcal{T}_k(\Omega_i)$ determined by the Gauss-Lobatto meshes on the single elements of $\mathcal{T}_i$ and interpolate ϑ_{E^j} at the GLL nodes: $\theta_{E^j} = I^h \vartheta_{E^j}$. The value of each θ_{E^j} at the vertices V^2 and V^3 is set equal to zero.

The functions θ_{E^j} are non negative and bounded by one: this proves the first of (30). By proceeding as for the proof of [8, Lem. 3.3.6] and using elementary properties of bilinear functions, we find

$$
\begin{array}{ll}
|\nabla \theta_{E^j}| \leq C/r, & y \geq 0, \\
|\nabla \theta_{E^j}| \leq C/H_i, & y \leq 0.
\end{array}
$$

This concludes the proof for an edge patch. For an unrefined patch the result can be found in [8, Lem. 3.3.6]. For a corner patch we note that we need consider only the two edges that do not lie on $\partial\Omega$ and the proof can be carried out in a similar way. $\square$

Lemma 7.7 *Let* θ_{E^j} *be the functions in Lemma 7.6, where* E^j *is an edge of the substructure* Ω_i. *Then, for every* $x \in \Omega_{i,h} \cup \Gamma_{i,h}$ *that is not a vertex of* Ω_i,

$$
\sum_j I^k(\theta_{E^j} u)(x) = \sum_j I^h(\theta_{E^j} u)(x) = u(x), \quad u \in X_i
$$

and

$$|I^k(\theta_{E^j}u)|^2_{1,\Omega_i} \leq C\,(1-\sigma)^{-3}\left(1+\log\left(\frac{k}{1-\sigma}\right)\right)^2 \|u\|^2_{1,\Omega_i}.$$

Proof. The proof is the same as that in [8, Lem. 3.3.7]. The only difference is that we do not work with just one spectral elements but on the whole patch Ω_i. As usual let $\mathcal{T}_k(\Omega_i)$ be the mesh obtained by considering the Gauss-Lobatto meshes on each element $K \in \mathcal{T}_i$. We only consider an edge patch which coincides with the reference element in full detail; see Figures 1 and 4. Let $K_V \in \mathcal{T}_i$ be the element that contains the vertices V^2 and V^3 and k_{V^l}, $l = 2,3$, the elements on the Gauss-Lobatto mesh $\mathcal{T}_k(\Omega_i)$, to which V^l belongs. We note that, after a possible translation and rotation, we have

$$k_{V^l} = (0,h_x) \times (0,h_y) = (0,Ck^{-2}(1-\sigma)) \times (0,Ck^{-2}).$$

and that $k_{V^l} \subset K_V$. We first consider the energy of $I^h(\theta_{E^j}u)$ on $\hat{k} = k_{V^l}$, $l = 2,3$. We first note that the nodal values of $I^h(\theta_{E^j}u)$ on $\hat{k}$ are 0, 0, $\theta_{E^j}(c')u(c) = u(c')$, and $\theta_{E^j}(d')u(d')$. Using Lemma 7.3 and the first of (30), we find

$$|I^h(\theta_{E^j}u)|^2_{1,\hat{k}} \leq \max\left\{\frac{h_x}{h_y},\frac{h_y}{h_x}\right\}(u(c')^2+u(d')^2) \leq C(1-\sigma)^{-1}\|u\|^2_{\infty,K_V}.$$

Lemma 7.5 thus yields

$$|I^h(\theta_{E^j}u)|^2_{1,k_{V^l}} \leq C(1-\sigma)^{-3}(1+\log k)\,\|u\|^2_{1,K_V}, \quad l=2,3. \qquad (31)$$

We now consider the elements $\hat{k} \in \mathcal{T}_k(\Omega_i)$ different from k_{V^1} or k_{V^2}. Using Lemma 7.2 and the second of (30), we have

$$\sum_{\hat{k}\subset\Omega_i} |I^h(\theta_{E^j}u)|^2_{1,\hat{k}} \leq C \sum_{\hat{k}\subset\Omega_i}(|u|^2_{1,\hat{k}}+r_{\hat{k}}^{-2}\|u\|^2_{0,\hat{k}}),$$

where $r_{\hat{k}}$ is the distance of the baricenter of $\hat{k}$ from the closest vertex of Ω_i that does not lie on $\partial\Omega$ and the sum is taken over elements in $\mathcal{T}_k(\Omega_i)$, k_{V^2} and k_{V^2} excluded. Using polar coordinates around V^2 and V^3, the last contribution can be bounded by

$$\sum_{\hat{k}\subset\Omega_i} r_{\hat{k}}^{-2}\|u\|^2_{0,\hat{k}} \leq C \int_{k^{-2}(1-\sigma)}^{C}\int_0^{2\pi} u^2\,\frac{r}{r^2}\,d\phi\,dr.$$

Using 7.5, we find

$$\sum_{\hat{k}\subset\Omega_i} |I^h(\theta_{E^j}u)|^2_{1,\hat{k}} \leq C|u|^2_{1,\Omega_i}+C(1-\sigma)^{-2}\left(1+\log\left(\frac{k}{1-\sigma}\right)\right)^2\|u\|^2_{1,\Omega_i}. \quad (32)$$

The proof is concluded by combining (31), (32), and Lemma 7.1.

For an unrefined patch the result can be found in [8, Lem. 3.3.7]. For a corner patch the proof can be carried out in a similar way. $\qquad\square$
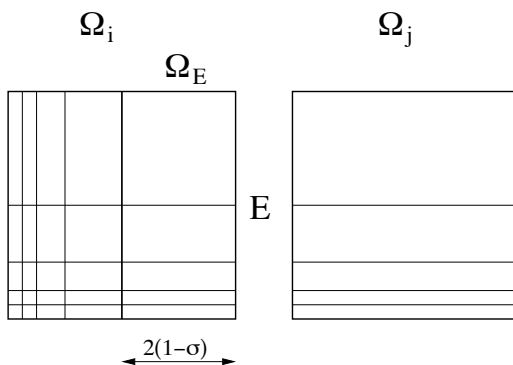
Figure 5: A corner and an edge patch which share an edge E. The edge patch Ω_j coincides with Ω_E after a stretching along the horizontal direction.

7.3 Comparison results

In the analysis of many iterative substructuring methods, it is necessary to compare the energy of discrete harmonic functions on different substructures that have the same trace on a common edge or the same value at a common vertex.

Lemmas 7.5 and 7.4 allow us to do so for vertex functions. Indeed they provide a trace and an extension theorem, respectively, for u and the boundary value $u(V)$.

If the local meshes are shape-regular and quasi-uniform, the comparison for edge functions on adjacent substructures, can also be made using a trace theorem (which is valid for general functions in H^1) and a stable extension. However, the existence of a stable extension for meshes that are not quasi-uniform or shape-regular is far from trivial. For this reason we will adopt a different strategy here, since the meshes considered are highly anisotropic but of a particular type.

We note that we only need to consider two cases: that of an edge shared by an unrefined and an edge patch, and by an edge and a corner patch. We only consider the latter case in full detail, since the former can be treated in exactly the same way. We consider the two substructures Ω_i and Ω_j in Figure 5, which share the edge E. We first consider Ω_i and suppose that it coincides with the reference square $\hat{Q}$. The edge E corresponds to $x = 1$. Let Ω_E be the layer of points in Ω_i within a distance $2(1 - \sigma)$ from E.

Lemma 7.8 *Let $u_E \in W_i$ be an edge function on Ω_i, i.e, a discrete harmonic function that vanishes on $\partial\Omega \setminus E$, and $\tilde{u}_E \in X_i$, such that*

   1. $\tilde{u}_E$ is equal to u_E on E and vanishes on $\partial\Omega_E \setminus E$;

2. $\tilde{u}_E$ is discrete harmonic in Ω_E;

3. $\tilde{u}_E$ vanishes in $\Omega_i \setminus \Omega_E$.

Then
$$|u_E|^2_{1,\Omega_i} \leq |\tilde{u}_E|^2_{1,\Omega_i} \leq \|\nabla \theta_{\sigma,E}\|^2_\infty \, |u_E|^2_{1,\Omega_i},$$

where $\theta_{\sigma,E} \in W^{1,\infty}(\Omega_i)$ is any function that is equal to one on E, vanishes in $\Omega_i \setminus \Omega_E$, and has values in $(0,1)$ in the rest of Ω_i. In particular we can find a function such that
$$\|\nabla \theta_{\sigma,E}\|_\infty \leq C(1-\sigma)^{-1}.$$

Proof. The first inequality is trivial and comes from the minimizing property of the harmonic extension in Lemma 6.1. For the second, we consider any function $\theta_{\sigma,E}$ that satisfies the given assumptions. Since $\tilde{u}_E$ is discrete harmonic in Ω_E, Lemma 6.1 ensures that

$$|\tilde{u}_E|^2_{1,\Omega_i} = |\tilde{u}_E|^2_{1,\Omega_E} \leq |I^k(\theta_{\sigma,E} u_E)|^2_{1,\Omega_E}.$$

It is then enough to find a bound for the piecewise bilinear function on the Gauss-Lobatto mesh $\mathcal{T}_k(\Omega_E)$, $I^h(\theta_{\sigma,E} u_E)$. This can be found using Lemma 7.2

$$|I^h(\theta_{\sigma,E} u_E)|^2_{1,\Omega_E} \leq C(|u|^2_{1,\Omega_E} + \|\nabla \theta_{\sigma,E}\|^2_\infty \|u\|^2_{0,\Omega_E}) \leq C\|\nabla \theta_{\sigma,E}\|^2_\infty \|u\|^2_{1,\Omega_i}.$$

Since u vanishes on $\partial \Omega_i \setminus E$, a Friedrichs inequality allows us to replace the H^1-norm with the seminorm.

A particular $\theta_{\sigma,E}$ can be chosen as a function that varies linearly in Ω_E along the horizontal direction, which decreases from one to zero in a layer of width $2(1-\sigma)$. □

The comparison result for edge functions can be then found by noting that we can map Ω_j and its mesh into Ω_E and the corresponding local mesh, by a simple dilation in the horizontal direction.

Theorem 7.2 *Let E be an edge that is common to Ω_i and Ω_j and $u_E \in W$ be a piecewise discrete harmonic function that is identically zero at all nodal points in $\Gamma_h \setminus E_h$. Then,*

$$c\,(1-\sigma)\,|u_E|^2_{1,\Omega_i} \leq |u_E|^2_{1,\Omega_j} \leq C(1-\sigma)^{-1}\,|u_E|^2_{1,\Omega_i}.$$

8   Proof of Assumption 6.1

We are now ready to give an upper bound for ω in Assumption 6.1. We note that functions in W_i vanish on Γ_h except at the nodal points in $\Gamma_{i,h}$ and their support is thus contained in the union of Ω_i and its neighboring substructures. In order to estimate ω we thus have to estimate the energy of $u \in W_i$ on these substructures in terms of the energy of $\mathcal{H}_i(\delta_i u)$ in Ω_i alone.

We first note that, by simple calculation, we have

$$\rho_j(\delta_i^\dagger(x))^2 = \rho_j \delta_i(x)^{-2} \le \min\{\rho_i, \rho_j\}, \qquad x \in \Gamma_{i,h}, \quad j \in \mathcal{N}_x. \qquad (33)$$

Let $u \in Range(\tilde{P}_i)$. We start with a substructure Ω_j that only has a vertex V in common with Ω_i. We note that u has only a vertex component on Ω_j, according to the decomposition (29). Using Lemma 7.4, we find

$$a_j(u,u) = \rho_j |u|_{1,\Omega_j}^2 \le C \rho_j (1-\sigma)^{-1} |u(V)|^2 \le C \rho_j \delta_i(V)^{-2} (1-\sigma)^{-1} |\delta_i(V) u(V)|^2.$$

We next apply Lemma 7.5 to the vertex component of $\mathcal{H}_i(\delta_i u)$:

$$\rho_i |\delta_i(V) u(V)|^2 \le C(1-\sigma)^{-2}(1+\log k) \, \rho_i \|\mathcal{H}_i(\delta_i u)\|_{1,\Omega_i}^2$$
$$= C(1-\sigma)^{-2}(1+\log k) \, (a_i(\mathcal{H}_i(\delta_i u), \mathcal{H}_i(\delta_i u)) + \rho_i H_i^{-2} \|\mathcal{H}_i(\delta_i u)\|_{0,\Omega_i}^2).$$

We note that the L^2 component in the last term can be bounded by the local bilinear form $a_i(\cdot, \cdot)$, thanks to a Poincaré inequality for floating subdomains (cf. (21)), or thanks to a Friedrichs inequality for substructures that touch $\partial\Omega$. Combining these two estimates and using (33), we find

$$a_j(u,u) \le C(1-\sigma)^{-3}(1+\log k) \, a_i(\mathcal{H}_i(\delta_i u), \mathcal{H}_i(\delta_i u)). \qquad (34)$$

We next consider a substructure Ω_j that shares an edge E with vertices V^1 and V^2. We note that on Ω_j, u can be decomposed as

$$u = u_{V^1} + u_{V^2} + u_E.$$

We have

$$a_j(u,u) = \rho_j |u|_{1,\Omega_j}^2 \le 3\rho_j(|u_{V^1}|_{1,\Omega_j}^2 + |u_{V^2}|_{1,\Omega_j}^2 + |u_E|_{1,\Omega_j}^2).$$

The vertex components can be bounded as before; cf. (34). For the edge component we first note that the function δ_i is constant at all nodal points inside E and is equal to $(\rho_i^\gamma + \rho_j^\gamma)/\rho_i^\gamma$. Using (33), we can then write

$$\rho_j |u_E|_{1,\Omega_j}^2 = \frac{\rho_j \rho_i^{2\gamma}}{\rho_i(\rho_i^\gamma + \rho_j^\gamma)^2} \, \rho_i |\mathcal{H}_j(\delta_i u_E)|_{1,\Omega_j}^2 \le \rho_i |\mathcal{H}_j(\delta_i u_E)|_{1,\Omega_j}^2.$$

Using Corollary 7.2 and Lemma 7.7 yields

$$|\mathcal{H}_j(\delta_i u_E)|_{1,\Omega_j}^2 \le C(1-\sigma)^{-1} |\mathcal{H}_i(\delta_i u_E)|_{1,\Omega_i}^2 \le C(1-\sigma)^{-4}\left(1 + \log\left(\frac{k}{1-\sigma}\right)\right)^2 \|u\|_{1,\Omega_i}^2.$$

Combining the last two estimates and using a Poincaré or a Friedrichs inequality, we find

$$\rho_j |u_E|_{1,\Omega_j}^2 \le C(1-\sigma)^{-4}\left(1 + \log\left(\frac{k}{1-\sigma}\right)\right)^2 a_i(\mathcal{H}_i(\delta_i u), \mathcal{H}_i(\delta_i u)). \qquad (35)$$

We finally need to consider the energy of u in Ω_i, $a_i(u, u)$. We note that we can decompose u on Ω_i according to (29). Each vertex and edge component can be bounded as before. Summing over i and the neighboring subdomains, we find

$$a(u, u) \leq C \, (1-\sigma)^{-4} \left(1 + \log \left(\frac{k}{1-\sigma} \right) \right)^2 \left(\sum_{E^{ij}} 1 + \sum_{V^{ik}} 1 \right) a_i(\mathcal{H}_i(\delta_i u), \mathcal{H}_i(\delta_i u)).$$

Since the partition $\mathcal{T}_m$ is shape-regular, the number of subdomains to which a vertex may belong is bounded. We finally obtain

$$\omega \leq C \, (1 - \sigma)^{-4} \left(1 + \log \left(\frac{k}{1-\sigma} \right) \right)^2.$$

Since in practice σ is bounded away from one, we obtain the same bound as for Neumann-Neumann methods for p finite element approximations on shape-regular meshes

$$\kappa(P_{NN}) \leq C \, (1 + \log k)^2;$$

see, e.g., [31]. We stress the fact that the constants in the last two estimates are independent of the coefficients ρ_i and the refinement level n (and thus of the aspect ratio of the mesh $\mathcal{T}_{bl}^{n,\sigma}$).

9 Proof of Assumption 6.2

The proof is very similar to that of Assumption 6.1. Before proceeding however we need an additional result which was not needed for Neumann-Neumann methods. A key step in the proof of the previous section is that the L^2-norm of functions in $Range(\tilde{P}_i) \subset W_i$ can be bounded by the H^1-seminorm (see, e.g., (34)), by using a Poincaré inequality (cf. (21)) for floating subdomains. Here however we work with functions in $Range(\tilde{S})$ and we need a similar property.

Lemma 9.1 *Let $u \in Range(\tilde{S})$. Then there is a constant independent of H_i and the local meshes such that*

$$\|u_i\|_{0,\Omega_i}^2 \leq C H_i^2 |u_i|_{1,\Omega_i}^2, \quad i = 1, \ldots, N.$$

Proof. The property is a consequence of Friedrichs inequality if Ω_i is not a floating subdomain. Since the columns of R span the null space of $\tilde{S}$, it is immediate to see that $u \in Range(\tilde{S})$ if and only if, for all floating subdomains Ω_i, $l_i(u_i) := k^{-1} r_i^T u_i = 0$. We recall that r_i is a vector consisting of ones. We also note that in our geometries corner and edge patches cannot be floating subdomains. The mesh on a floating substructure is thus shape-regular and quasi-uniform. In particular, for our prototype meshes floating subdomains can only be shape-regular spectral elements, possibly affinely mapped; cf. Figure 2.

Recalling the expression for the Gauss-Lobatto weights (see [5, Th. 4.5]) and using (11), we find, for $u_i \in W_i$,

$$|l_i(u_i)| = |k^{-1} r_i^T u_i| \le C_i' \|u_i\|_{0,\partial\Omega_i}.$$

The functional $l_i(\cdot)$ can thus be extended as a continuous linear functional, still denoted by $l_i(\cdot)$, to the whole of $L^2(\partial\Omega_i)$. Since, if u_i is constant on $\partial\Omega_i$, then $l_i(u_i) = 0$ if and only if $u_i = 0$, [29, Th. 7.1] ensures that

$$\|u_i\|_{0,\Omega_i}^2 \le CH_i^2 |u_i|_{1,\Omega_i}^2 + C_i l_i(u_i)^2, \quad u_i \in H^1(\Omega_i),$$

where C_i only depends on the shape and size of Ω_i, and C only on its shape. This concludes the proof. $\square$

Let now $u \in Range(\tilde{S})$. An expression for $P_D u$ can be found in [19]:

$$(P_D u(x))_i = v_i(x) = \sum_{j \in \mathcal{N}_x} \delta_j^\dagger(x)(u_i(x) - u_j(x)), \qquad x \in \Gamma_{i,h}, \quad u \in \tilde{W}. \quad (36)$$

Here $\mathcal{N}_x$ is again the set of indices of the subregions that have x on their boundaries. We recall that $\delta_j^\dagger$ is constant on each edge of Γ_i. It is therefore natural to decompose v_i according to (29). However, since we need to consider traces from different subdomains and then extend them into one substructure, we introduce a different notation for (29):

$$v_i = \sum_k P_{E^{ik}}(v_i) + \sum_l P_{V^{il}}(v_i). \quad (37)$$

We assume that the edge E^{ik} is shared by Ω_i and Ω_k. In order to construct $P_{E^{ik}}(w_j)$, for $w_j \in W_j$ and $j = i, k$, we first restrict w_j to E^{ik} and then extend it harmonically in Ω_i. Similarly, in order to construct $P_{V^{il}}(w_j)$, for $w_j \in W_j$ and $j \in \mathcal{N}_{V^{il}}$, we take the value $w_j(V^{il})$ and then extend it harmonically in Ω_i as a vertex function.

We now bound each term in (37) separately. We start by an edge component $P_{E^{ik}}(v_i)$ and note that in the sum in (36) there is only one non-vanishing term, corresponding to $j = k$. For every $x \in E_h^{ik}$, we have $\delta_j^\dagger(x) = \rho_j^\gamma/(\rho_j^\gamma + \rho_i^\gamma)$, and thus

$$|P_{E^{ik}}(v_i)|_{S_i}^2 = \rho_i |P_{E^{ik}}(v_i)|_{1,\Omega_i}^2 \le 2 \left(\frac{\rho_j^\gamma}{\rho_j^\gamma + \rho_i^\gamma} \right)^2 (\rho_i |P_{E^{ik}}(u_i)|_{1,\Omega_i}^2 + \rho_i |P_{E^{ik}}(u_k)|_{1,\Omega_i}^2).$$

Using Corollary 7.2 and (33), we find

$$|P_{E^{ik}}(v_i)|_{S_i}^2 \le (\rho_i |P_{E^{ik}}(u_i)|_{1,\Omega_i}^2 + \rho_k (1-\sigma)^{-1} |P_{E^{ki}}(u_k)|_{1,\Omega_k}^2).$$

The stability result in Lemma 7.7 and the bound in Lemma 9.1 yield

$$|P_{E^{ik}}(v_i)|_{S_i}^2 \le C (1-\sigma)^{-4} \left(1 + \log\left(\frac{k}{1-\sigma} \right) \right)^2 (a_i(u_i, u_i) + a_k(u_k, u_k)). \quad (38)$$

We now consider a vertex component $P_{V^{il}}(v_i)$ and note that there are $(\mathcal{N}_{V^{il}} - 1)$ non-vanishing terms in the sum in (36). We can thus write

$$P_{V^{il}}(v_i) = P_{V^{il}}\left(\sum_{\substack{j \in \mathcal{N}_{V^{il}} \\ j \neq i}} \delta_j^\dagger(u_i - u_j)\right) = \sum_{\substack{j \in \mathcal{N}_{V^{il}} \\ j \neq i}} \delta_j^\dagger(V^{il})\, P_{V^{il}}(u_i - u_j).$$

Each component can be bounded using Corollary 7.1. Noting that the number of substructures in $\mathcal{N}_{V^{il}}$ is uniformly bounded since the macromesh $\mathcal{T}_m$ is shape-regular, we find

$$\rho_i |P_{V^{il}}(v_i)|_{1,\Omega_i}^2 \leq C(1-\sigma)^{-1} \sum_{\substack{j \in \mathcal{N}_{V^{il}} \\ j \neq i}} \delta_j(V^{il})^{-2}(\rho_i |u_i(V^{il})|^2 + \rho_i |u_j(V^{il})|^2).$$

Using then (33) and Lemma 7.5, we obtain

$$\rho_i |P_{V^{il}}(v_i)|_{1,\Omega_i}^2 \leq C(1-\sigma)^{-1}(1+\log k) \sum_{j \in \mathcal{N}_{V^{il}}} (a_j(u_j, u_j) + \rho_j H_j^{-2} \|u_j\|_{0,\Omega_j}^2)$$

where we have used again the property that the number of terms in the sum is uniformly bounded. Applying Lemma 9.1 yields

$$|P_{V^{il}}(v_i)|_{S_i}^2 \leq C(1-\sigma)^{-1}(1+\log k) \sum_{j \in \mathcal{N}_{V^{il}}} a_j(u_j, u_j). \tag{39}$$

We next combine (37), (38), and (39) and obtain

$$|v_i|_{S_i}^2 \leq C(1-\sigma)^{-4}\left(1 + \log\left(\frac{k}{1-\sigma}\right)\right)^2 \sum_{V^{il}} \sum_{j \in \mathcal{N}_{V^{il}}} a_j(u_j, u_j),$$

where we have used the fact that if two substructures share an edge they also share its end points, which must be vertices of the two substructures. Summing then over the substructures $\{\Omega_i\}$ and using the property that the number of substructures in each $\mathcal{N}_{V^{il}}$ is uniformly bounded, we find

$$|v|_{\tilde{S}}^2 \leq \omega |u|_{\tilde{S}}^2,$$

with

$$\omega \leq C(1-\sigma)^{-4}\left(1 + \log\left(\frac{k}{1-\sigma}\right)\right)^2.$$

We remark that we find the same bound as for the Neumann-Neumann operator:

$$\kappa(PM^{-1}P^T F) \leq C(1+\log k)^2,$$

if σ is bounded away from one, as it is always the case in practical applications. As before the constants in the last two estimates are independent of the coefficients ρ_i and the refinement level n (and thus of the aspect ratio of the mesh $\mathcal{T}_{bl}^{n,\sigma}$).
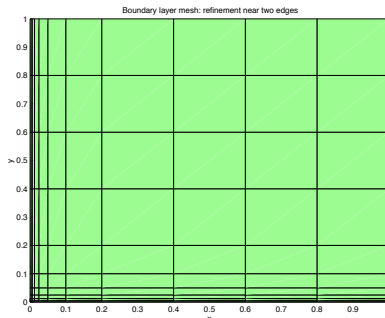
Figure 6: Boundary layer mesh with refinement near two edges with mesh grading factors $\sigma_x = 0.5$ and $\sigma_y = 0.5$. The unrefined grid is a cartesian grid of size $N_x \times N_y = 5 \times 5$.

10 Numerical results

The purpose of this section is to present two sets of numerical experiments in order to show that the theoretical bounds for the condition number for the model problem (2) derived in this paper appear to hold for the singularly-perturbed problem (1). An extensive numerical study is presented elsewhere; see [40].

We only consider a Balancing Neumann-Neumann method for approximations on the unit square $\Omega = (0,1)^2$. We choose $\rho \equiv 1$ and the right-hand side $f \equiv 1$. The macromesh $\mathcal{T}_m$ consists of 5×5 substructures. Geometric refinement is performed towards the two edges $x = 0$ and $y = 0$, with $\sigma = 0.5$; see Figure 6.

We first consider the model problem (2). Given a polynomial degree k, we choose $n = k$ as is required for robust exponential convergence; see, e.g., [2, 4]. The conjugate gradient iteration is stopped after a reduction of the Euclidean norm of the initial residual of 10^{-14}. Table 1 shows the iteration count, the estimated maximum and minimum eigenvalues, and the condition number for different values of k. We note that the minimum eigenvalue is equal to one; see Lemma 6.2. In addition a moderate growth of the maximum eigenvalue is observed with k; such growth is consistent with the quadratic bound in Lemma 6.3.

We next consider the singularly-perturbed problem (1). We note that the right-hand side f is not consistent with homogeneous Dirichlet conditions. For a given ϵ, we choose

$$n = \left\lfloor \frac{\log(\sqrt{\epsilon}/H)}{\log \sigma} \right\rfloor + 1, \quad k = n,$$

NN, $N_x \times N_y = 5 \times 5$ substructures				
k	It	λ_{max}	λ_{min}	κ
2	12	1.5953	1	1.5953
3	16	2.2623	1	2.2623
4	19	2.9932	1	2.9932
5	22	3.7629	1	3.7629
6	23	4.5352	1	4.5352
7	25	5.2641	1	5.2641
8	25	5.9242	1	5.9242
9	26	6.5088	1	6.5088
10	27	7.0275	1	7.0275
11	27	7.4915	1	7.4915
12	27	7.9135	1	7.9135

Table 1: Laplace problem in the unit square. Conjugate Gradient method with Neumann-Neumann preconditioner: iteration count, maximum and minimum eigenvalues, and condition number.

where $\lfloor x \rfloor$ denotes the integer part of x. These conditions ensure that the width of the thinnest layer, $H\sigma^n$, is comparable to the size of the boundary layer, $\sqrt{\epsilon}$, as is required for boundary layer resolution (see [28, 37, 38]) and that n is comparable to k, as is required for singularities. Table 2 shows the polynomial degree, the iteration count, the maximum and minimum eigenvalues, and the condition number for different values of ϵ. We note that the minimum eigenvalue is equal to one; see Lemma 6.2. In addition the maximum eigenvalue and the condition number is bounded independently of ϵ. We also show results for Conjugate Gradient applied to the original Schur complement system. We note that for $\epsilon = 0$ the stiffness matrix A reduces to the mass matrix but that mass matrices arising from spectral elements are not necessarily uniformly well-conditioned even for shape-regular meshes, as can be seen using the first property in Lemma 7.3 and the equivalence in Lemma 7.1. This is consistent with the bounds found for the eigenvalues of S.

11   Concluding remarks

As mentioned earlier, this is only a first, preliminary work and many important issues still need to be addressed.

Our analysis is restricted to approximations that employ nodal basis functions on the Gauss-Lobatto nodes. While for three-dimensional shape-regular meshes good performance of iterative substructuring methods is ensured only if these basis functions are employed, for two dimensional problems other choices

$N_x \times N_y = 5 \times 5$ substructures									
		No preconditioning				NN			
ε	k	It	λ_{max}	λ_{min}	κ	It	λ_{max}	λ_{min}	κ
1	2	27	5.55E+00	2.67E-01	2.08E+01	9	1.197	1	1.197
10^{-1}	2	26	5.62E-01	3.77E-02	1.49E+01	9	1.189	1	1.189
10^{-2}	2	40	1.33E-01	9.13E-03	1.46E+01	9	1.255	1	1.255
10^{-3}	3	42	2.39E-02	9.44E-04	2.53E+01	8	1.179	1	1.179
10^{-4}	5	81	8.26E-03	5.53E-05	1.49E+02	6	1.112	1	1.112
10^{-5}	6	82	1.61E-03	8.37E-06	1.92E+02	4	1.021	1	1.021
10^{-6}	8	128	6.26E-04	9.54E-07	6.56E+02	3	1.003	1	1.003
10^{-7}	10	183	2.48E-04	1.43E-07	1.74E+03	2	1.000	1	1.000
10^{-8}	11	213	8.24E-05	3.85E-08	2.14E+03	1	1	1	1

Table 2: Singularly-perturbed problem in the unit square. Conjugate Gradient method for the Schur complement system without preconditioning and with Neumann-Neumann preconditioner: polynomial degree, iteration count, maximum and minimum eigenvalues, and condition number.

are possible. In particular, piecewise linear nodal basis functions and tensor products of integrated Legendre polynomials can be employed (see, e.g, [36, Sect. 3.1.6 and 4.4.2]): they are widely used in hp codes since they have the advantage, for instance, that they provide hierarchic basis functions and that different polynomial degrees can be employed for internal and side functions. For such approximations, a stability result for edge components, as in Lemma 7.7, is proven using an inverse estimate for the trace on an edge and a stable extension into the substructures; cf., e.g., [3, Th. 6.6]. However, since we are lacking such extension on our anisotropic meshes, we cannot in general work with trace spaces and we are forced to work with the partition of unity functions $\{\theta_E\}$ and interpolation on the Gauss-Lobatto mesh.

The Dirichlet and Neumann problems that we need to solve (cf. S_i and $S_i^\dagger$) can be potentially very large if a truly hp version is employed. On the other hand, our algorithms appear to require shape-regular substructures. Approximate local solvers can be employed for iterative substructuring methods (see, e.g., [10, 18]) and some have been proposed in [21] for hp approximations. In our case, we believe that the tensor product structure of corner and edge patches can be exploited, but this is left to a future work.

We believe that the analysis and/or the development of iterative substruc-

turing methods for general meshes with hanging nodes still need to be fully addressed. The algorithms in [30] for instance can certainly be employed when hanging nodes are present on the interface Γ and the analysis can be carried out using stable extensions for meshes with hanging nodes (see, e.g., [36, Sect. 4.6.3]). However there is no straightforward way of defining Neumann-Neumann or FETI algorithms in this case; see Remark 6.1.

The development and analysis of Neumann-Neumann and FETI methods for three dimensional approximations on geometrically refined meshes remain an open problem.

Acknowledgments

References

[1] Mark Ainsworth. A preconditioner based on domain decomposition for hp–FE approximation on quasi–uniform meshes. *SIAM J. Numer. Anal.*, 33:1358–1376, 1996.

[2] B. Andersson, U. Falk, I. Babuška, and T. von Petersdorff. Reliable stress and fracture mechanics analysis of complex aircraft components using a hp–version FEM. *Int. J. Numer. Meth. Eng.*, 38(13):2135–2163, 1995.

[3] Ivo Babuška, Alan Craig, Jan Mandel, and Juhani Pitkäranta. Efficient preconditioning for the p-version finite element method in two dimensions. *SIAM J. Numer. Anal.*, 28(3):624–661, 1991.

[4] Ivo Babuška and Benqi Guo. Approximation properties of the hp–version of the finite element method. *Comp. Methods Appl. Mech. Eng.*, 133:319–346, 1996.

[5] Christine Bernardi and Yvon Maday. Spectral methods. In *Handbook of Numerical Analysis, Vol. V, Part 2*, pages 209–485. North-Holland, Amsterdam, 1997.

[6] Ion Bica. *Iterative substructuring algorithms for the p–version finite element method for elliptic problems*. PhD thesis, Courant Institute, New York University, 1997.

[7] Claudio Canuto. Stablization of spectral methods by finite element bubble functions. *Comput. Methods Appl. Mech. Engrg*, 116:13–26, 1994. Proceedings of ICOSAHOM 92, a conference held in Montpellier, France, June 1992.

34

[8] Mario A. Casarin. *Schwarz Preconditioners for Spectral and Mortar Finite Element Methods with Applications to Incompressible Fluids.* PhD thesis, Courant Institute of Mathematical Sciences, March 1996. Tech. Rep. 717, Department of Computer Science, Courant Institute.

[9] Maksymilian Dryja, Marcus V. Sarkis, and Olof B. Widlund. Multilevel Schwarz methods for elliptic problems with discontinuous coefficients in three dimensions. *Numer. Math.*, 72(3):313–348, 1996.

[10] Maksymilian Dryja, Barry F. Smith, and Olof B. Widlund. Schwarz analysis of iterative substructuring algorithms for elliptic problems in three dimensions. *SIAM J. Numer. Anal.*, 31(6):1662–1694, December 1994.

[11] Maksymilian Dryja and Olof B. Widlund. Schwarz methods of Neumann-Neumann type for three-dimensional elliptic finite element problems. *Comm. Pure Appl. Math.*, 48(2):121–155, February 1995.

[12] Charbel Farhat, Michel Lesoinne, Patrick LeTallec, Kendall Pierson, and Daniel Rixen. FETI-DP: a dual-primal unified FETI method. I. A faster alternative to the two-level FETI method. *Internat. J. Numer. Methods Engrg.*, 50(7):1523–1544, 2001.

[13] Charbel Farhat and François-Xavier Roux. Implicit parallel processing in structural mechanics. In J. Tinsley Oden, editor, *Computational Mechanics Advances*, volume 2 (1), pages 1–124. North-Holland, 1994.

[14] Charbel Farhat and Francois-Xavier Roux. A Method of Finite Element Tearing and Interconnecting and its Parallel Solution Algorithm. *Int. J. Numer. Meth. Engng.*, 32:1205–1227, 1991.

[15] Benqi Guo and Weiming Cao. A preconditioner for the *hp*–version of the finite element method in two dimensions. *Numer. Math.*, 75:59–77, 1996.

[16] Benqi Guo and Weiming Cao. Additive Schwarz methods for the *hp* version of the finite element method in two dimensions. *SIAM Journal on Scientific Computing*, 18(5):1267–1288, 1997.

[17] Benqi Guo and Weiming Cao. An additive Schwarz method for the *hp*–version of the finite element method in three dimensions. *SIAM J. Numer. Anal.*, 35:632–654, 1998.

[18] Axel Klawonn and Olof B. Widlund. A domain decomposition method with Lagrange multipliers and inexact solvers for linear elasticity. *SIAM J. Sci. Comput.*, 22(4):1199–1219, October 2000.

[19] Axel Klawonn and Olof B. Widlund. FETI and Neumann-Neumann iterative substructuring methods: connections and new results. *Comm. Pure Appl. Math.*, 54(1):57–90, 2001.

[20] Axel Klawonn, Olof B. Widlund, and Maksymilian Dryja. Dual-Primal FETI methods for three-dimensional elliptic problems with heterogeneous coefficients. Technical Report 815, Department of Computer Science, Courant Institute, April 2001. Submitted to SIAM J. on Num. Anal.

[21] V. Korneev, J.E. Flaherty, J.T. Oden, and J. Fish. Additive Schwarz algorithms for solving hp-version finite element systems on triangular meshes. *SIAM J. Numer. Anal.*, 1998. submitted.

[22] Jan Mandel. Iterative methods for p–version finite elements: preconditioning thin solids. *Comp. Methods Appl. Mech. Eng.*, 133:247–257, 1996.

[23] Jan Mandel and Marian Brezina. Balancing domain decomposition for problems with large jumps in coefficients. *Math. Comp.*, 65:1387–1401, 1996.

[24] Jan Mandel and G. Scott Lett. Domain decomposition preconditioning for p–version finite elements with high aspect ratios. *Appl. Num. Math.*, 8:411–425, 1991.

[25] Jan Mandel and Radek Tezaur. Convergence of a substructuring method with Lagrange multipliers. *Numer. Math.*, 73:473–487, 1996.

[26] Jan Mandel and Radek Tezaur. On the convergence of a dual-primal substructuring method. *Numer. Math.*, 88(3):543–558, January 2001.

[27] J. M. Melenk. On condition numbers in hp-FEM with Gauss-Lobatto-based shape functions. *J. Comput. Appl. Math.*, 139(1):21–48, 2002.

[28] Jens Markus Melenk and Christoph Schwab. hp–FEM for reaction–diffusion equations. I: Robust exponential convergence. *SIAM J. Numer. Anal.*, 35:1520–1557, 1998.

[29] Jindřich Nečas. *Les méthodes directes en théorie des équations elliptiques.* Academia, Prague, 1967.

[30] J. T. Oden, Abani Patra, and Yusheng Feng. Parallel domain decomposition solver for adaptive hp finite element methods. *SIAM J. Numer. Anal.*, 34:2090–2118, 1997.

[31] Luca F. Pavarino. Neumann-Neumann algorithms for spectral elements in three dimensions. *RAIRO Mathematical Modelling and Numerical Analysis*, 31:471–493, 1997.

[32] Luca F. Pavarino. Neumann-Neumann algorithms for spectral elements in three dimensions. *RAIRO Mathematical Modelling and Numerical Analysis*, 31:471–493, 1997.

[33] Alfio Quarteroni and Alberto Valli. *Numerical Approximation of Partial Differential Equations*. Springer-Verlag, Berlin, 1994.

[34] Marcus V. Sarkis. *Schwarz Preconditioners for Elliptic Problems with Discontinuous Coefficients Using Conforming and Non-Conforming Elements*. PhD thesis, Courant Institute, New York University, September 1994. TR671, Department of Computer Science, New York University, URL: `file://cs.nyu.edu/pub/tech-reports/tr671.ps.Z`.

[35] Dominik Schötzau, Christoph Schwab, and Rolf Stenberg. Mixed hp–FEM on anisotropic meshes II: Hanging nodes and tensor products of boundary layer meshes. *Numer. Math.*, 83:667–697, 1999.

[36] Christoph Schwab. *p– and hp– finite element methods*. Oxford Science Publications, 1998.

[37] Christoph Schwab and Manil Suri. The p and hp version of the finite element method for problems with boundary layers. *Math. Comp.*, 65:1403–1429, 1996.

[38] Christoph Schwab, Manil Suri, and Christos A. Xenophontos. The hp–FEM for problems in mechanics with boundary layers. *Comp. Methods Appl. Mech. Eng.*, 157:311–333, 1998.

[39] Barry F. Smith, Petter E. Bjørstad, and William D. Gropp. *Domain Decomposition: Parallel Multilevel Methods for Elliptic Partial Differential Equations*. Cambridge University Press, 1996.

[40] Andrea Toselli and Xavier Vasseur. Robust Neumann-Neumann and FETI methods for hp-approximations on geometrically refined boundary layer meshes in two dimensions: numerical results. In preparation.

Research Reports

No.	Authors	Title
02-15	A. Toselli, X. Vasseur	Neumann-Neumann and FETI preconditioners for hp-approximations on geometrically refined boundary layer meshes in two dimensions
02-14	Th.P. Wihler	Locking-Free DGFEM for Elasticity Problems in Polygons
02-13	S. Beuchler, R. Schneider, C. Schwab	Multiresolution weighted norm equivalences and applications
02-12	M. Kruzik, A. Prohl	Macroscopic modeling of magnetic hysteresis
02-11	A.-M. Matache, C. Schwab, T. von Petersdorff	Fast deterministic pricing of options on Lévy driven assets
02-10	D. Schötzau, C. Schwab, A. Toselli	Mixed hp-DGFEM for incompressible flows
02-09	Ph. Frauenfelder, Ch. Lage	Concepts - An object-oriented software package for partial differential equations
02-08	A.-M. Matache, J.M. Melenk	Two-Scale Regularity for Homogenization Problems with Non-Smooth Fine Scale Geometry
02-07	G. Schmidlin, C. Lage, C. Schwab	Rapid solution of first kind boundary integral equations in $\mathbb{R}^3$
02-06	M. Torrilhon	Exact Solver and Uniqueness Conditions for Riemann Problems of Ideal Magnetohydrodynamics
02-05	C. Schwab, R.-A. Todor	Sparse Finite Elements for Elliptic Problems with Stochastic Data
02-04	R. Jeltsch, K. Nipp	CSE Program at ETH Zurich: Are we doing the right thing?
02-03	L. Diening, A. Prohl, M. Ruzicka	On Time-Discretizations for Generalized Newtonian Fluids
02-02	A. Toselli	hp Discontinuous Galerkin Approximation for the Stokes Problem
02-01	F.M. Buchmann, W.P. Petersen	Solving Dirichlet problems numerically using the Feynman-Kac representation
01-09	A.-M. Matache	Sparse Two-Scale FEM for Homogenization Problems
01-08	C. Lasser, A. Toselli	Convergence of some two-level overlapping domain decomposition preconditioners with smoothed aggregation coarse space
01-07	T. von Petersdorff, C. Schwab	Wavelet-discretizations of parabolic integro-differential equations